JJEES

Volume 3, Number 1, June, 2010
ISSN 1995-6681
Pages 25- 36

Jordan Journal of Earth and Environmental Sciences

Paleostress Analysis of the Cretaceous Rocks in Northern Jordan

Nuha Al Khatib [a], Mohammad atallah [a], Abdullah Diabat [b,*]

[a] Department of Earth and Environmental Sciences, Yarmouk University Irbid-Jordan

[b] Institute of Earth and Environmental Sciences, Al al-Bayt University, Mafraq- Jordan

Abstract

Stress inversion of 747 fault- slip data was performed using an improved Right-Dihedral method, followed by rotational optimization (WINTENSOR Program, Delvaux, 2006). Fault-slip data including fault planes, striations and sense of movements, are obtained from the quarries of Turonian Wadi As Sir Formation , and distributed over 14 stations in the study area of Northern Jordan. The orientation of the principal stress axes (σ_1, σ_2, and σ_3) and the ratio of the principal stress differences (R) show that σ_1 (SHmax) and σ_3 (SHmin) are generally sub-horizontal and σ_2 is sub-vertical in 9 of 15 paleostress tensors, which are belonging to a major strike-slip system with σ_1 swinging around NNW direction. Four stress tensors show σ_2 (SHmax), σ_1 vertical and σ_3 are NE oriented. This situation is explained as permutation of stress axes σ_1 and σ_2 that occur during tectonic events. The new paleostress results show three paleostress regimes that belong to two main stress fields. The first is characterized by E-W to WNW-ESE compression and N-S to NNE –SSW extension. This stress field is associated with the formation of the Syrian Arc fold belt started in the Turonian. The second paleostress field is characterized by NW-SE to NNW-SSE compression and NE-SW to ENE-WSW extension. It is related to Middle Miocene – Recent sinistral movement along the Dead Sea transform and the opening of the Red Sea.

Keywords: Paleostress, Turonian- Miocene, Northern Jordan.

1. Introduction

The major structures in the Levant are the Dead Sea transform (DST) and the Syrian Arc belt (SAB). The Dead Sea transform extends from the Gulf of Aqaba in the south to the Taurus mountains in Turkey in the north. It separates the Arabian plate from Sinai sub-plate and connects the Red Sea spreading center with the Alpine orogeny in the north (Fig. 1). The DST was formed as a result of the northward sinistral movement of the Arabian plate associated with the opening of the Red Sea. The movement started in the Miocene and is still active in the present times. The Syrian arc is a system of fold belts extending from Sinai in the southwest to central Syria in the northeast (Fig. 1). This folding was formed in two phases. The first phase formed in the Turonian-Maestrichtian and the second phase in the Oligocene. The structural pattern of Jordan was affected since the Late Cretaceous by the movement along the DST and the formation of the SAB . The regional tectonics of the continental part of the Arabian plate including Jordan has been studied through macrostructures by many authors (e.g., Burdon 1959; Bender 1968; Mikbel and Zacher 1981; Quennell 1983; Mikbel 1986; Atallah 1992). Few analyses have been focusing, however, on the regional tectonics based on mesostructures in Jordan (e.g., Salameh and Zacher 1982; Diabat 1999, 2002; Zain Eldeen et al.,2002; Diabat et al., 2003., 2004; Diabat and Masri 2005). The relative motion across the DST has been estimated both by regional plate motion models and local slip rate considerations. The regional plate motion studies used the fault orientation , additional local observations, and constraints from the motion of neighboring plates to estimate 5- 10 mm/ yr of relative motion across the DST (e.g., Garfunkel, 1981; Joffe and Garfunkel, 1987; Chu and Gordon, 1998). Local geologic and seismic studies, which estimate the slip rate across the DST, yielded a wider range of relative motion estimates, from 1 to 10 mm/ yr (e.g., Freund et al., 1968 ; Mckenzie et al., 1970; Ben Avraham et al., 1979; Shapira and Hofstetter, 1993; Klinger et al., 2000a, 2000b). Generally, seismic estimates show a rate of only 1- 4 mm/ yr, geomorphologic estimates are in the range of 3- 7 mm/ yr, whereas long-term geological estimates are in the range of 6- 10 mm/ yr. Space geodetic technologies, in particular GPS, providing the first direct estimates of current plate motion in the eastern Mediterranean, estimated the current slip rate across the DST as 3.3 +- 0.4 mm/ yr.

Mesostructures are considered to be accurate indicators of the paleostress and strain orientation (Angelier, 1979, 1989, 1994; Delvaux et al., 1995, 1997).

Horizontal stylolites in Jordan were measured and described for the first time by Salameh and Zacher (1982), when they studied the relationship between stylolites and

* Corresponding author. abdullahdiabat@yahoo.ca

paleostresses. Zain Eldeen et al (2002) studied the tectonic evolution of the Wadi Araba segment (the southern part of the DST), based on fault slip data. Diabat (1999) and Diabat et al. (2004) studied the paleostresses at the eastern rim of the DST. The study represents the first results of the paleostresses in Jordan based on fault slip data (Slickenside analysis). Their results summarize the stress field east of the DST in two compression stress systems; the NNW-SSW Dead Sea system (DSS), and the Syrian Arc system (SAS).

The area of investigation is located in the northern part of Jordan (Figs1,2 and 3). It includes Al Husn, Shatana, Kitim, Deyr Yusif, Eshtafaina, and Thaghret Asfour, where Upper Cretaceous (Turonian) rocks are well exposed in many quarries. This gives a good opportunity for measuring fault slip data.

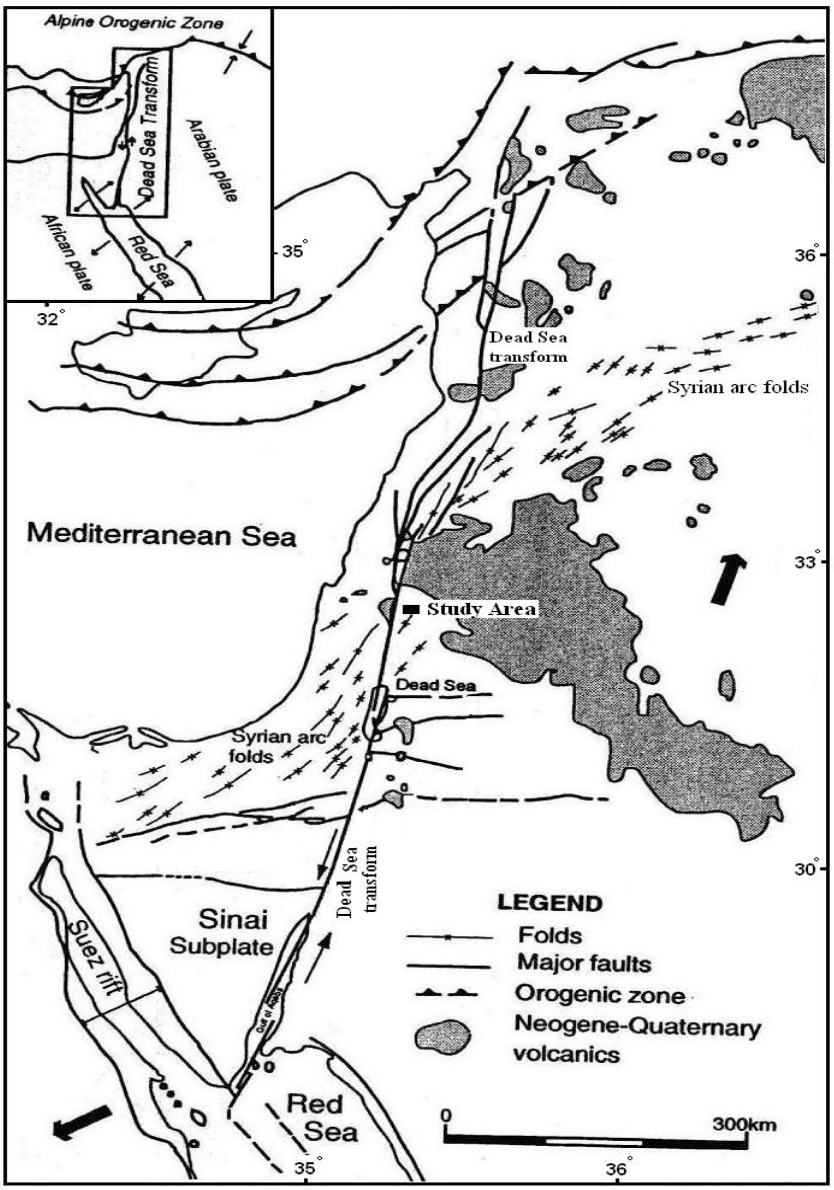

Fig. 1. Tectonic setting of the Dead Sea transform and the Syrian Arc, showing the study area (modified after Garfunkel, 1981).

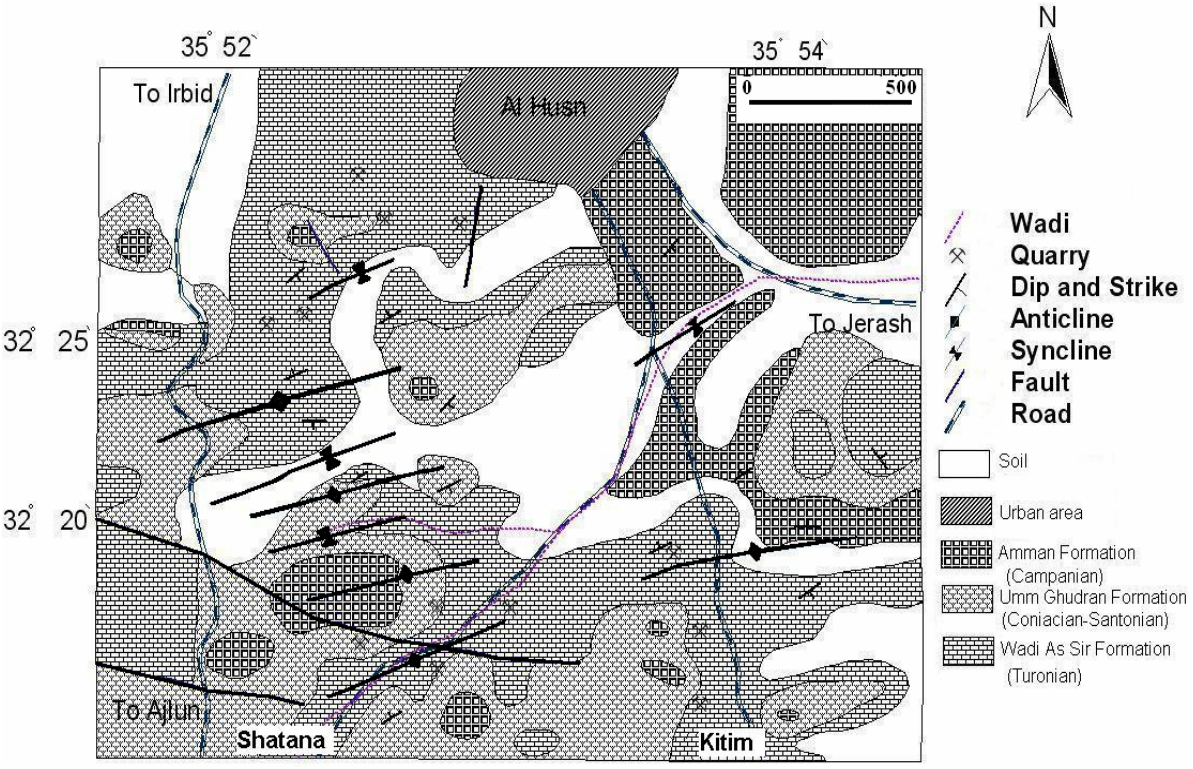

Fig. 2.a (1): Geological map of Al Husn area.

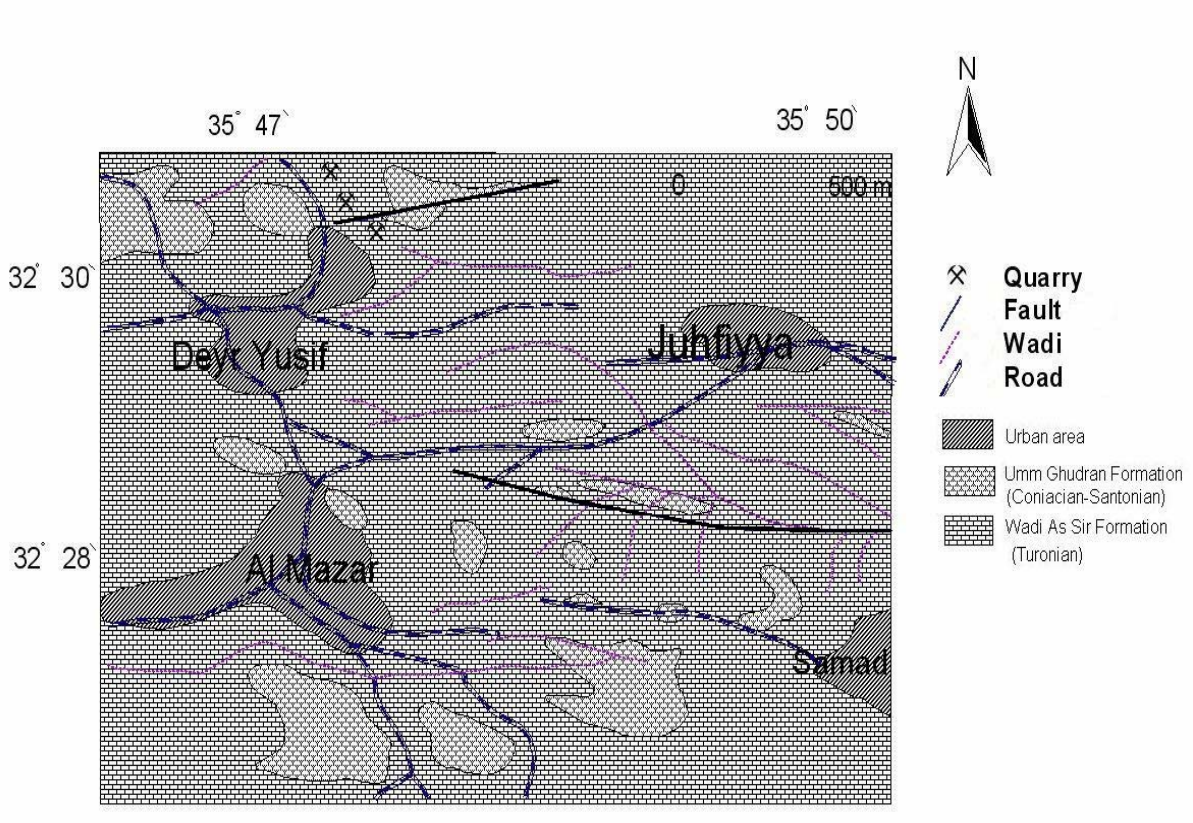

Fig. 2.a (2): Geological map of Deyr Yusif area.

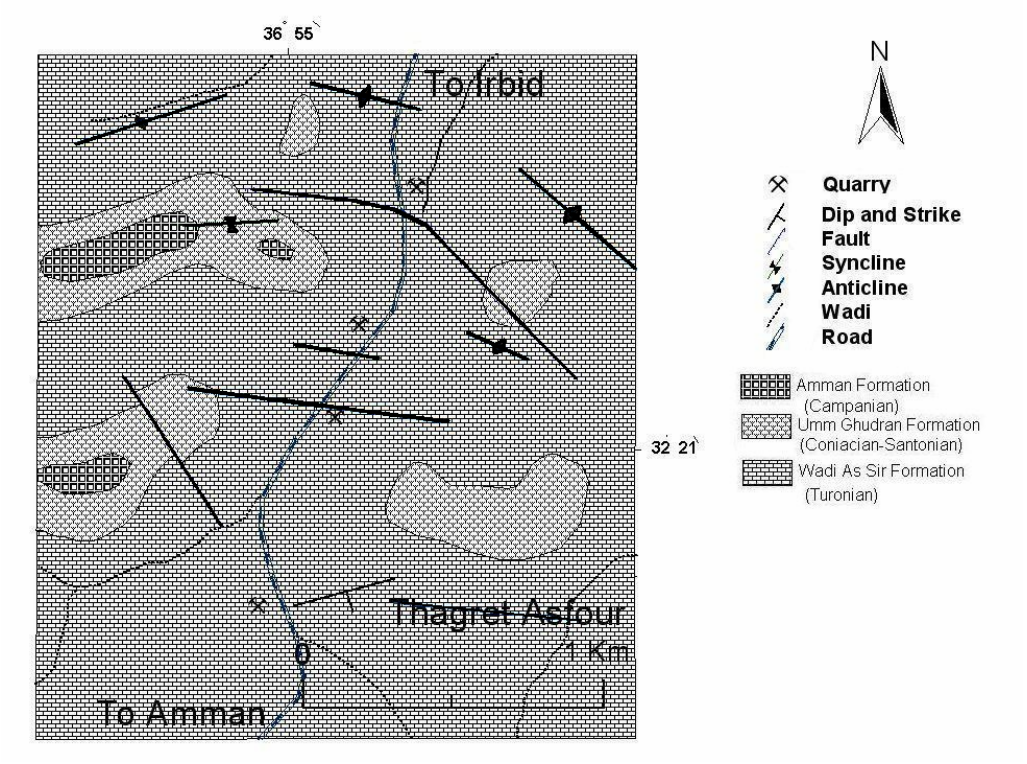

Fig 2. b (1) : Geological map of Thagret Asfour area.

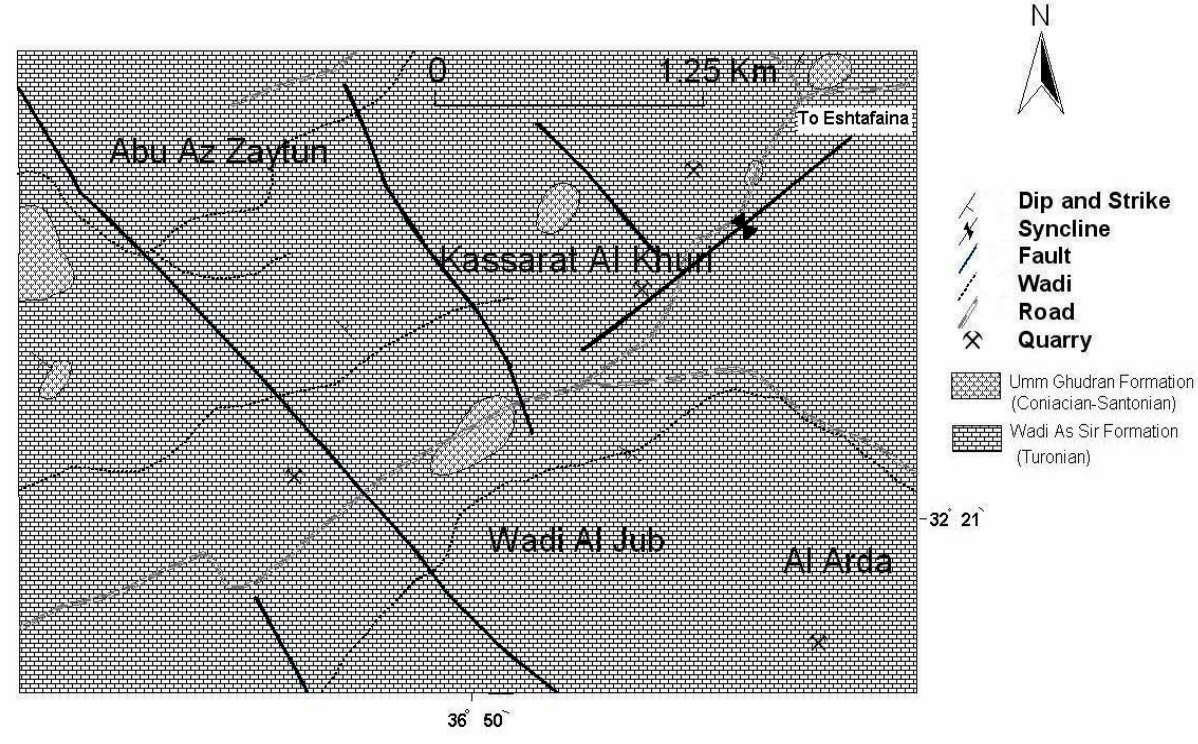

Fig 2. b (2) : Geological map of Eshtafaina area

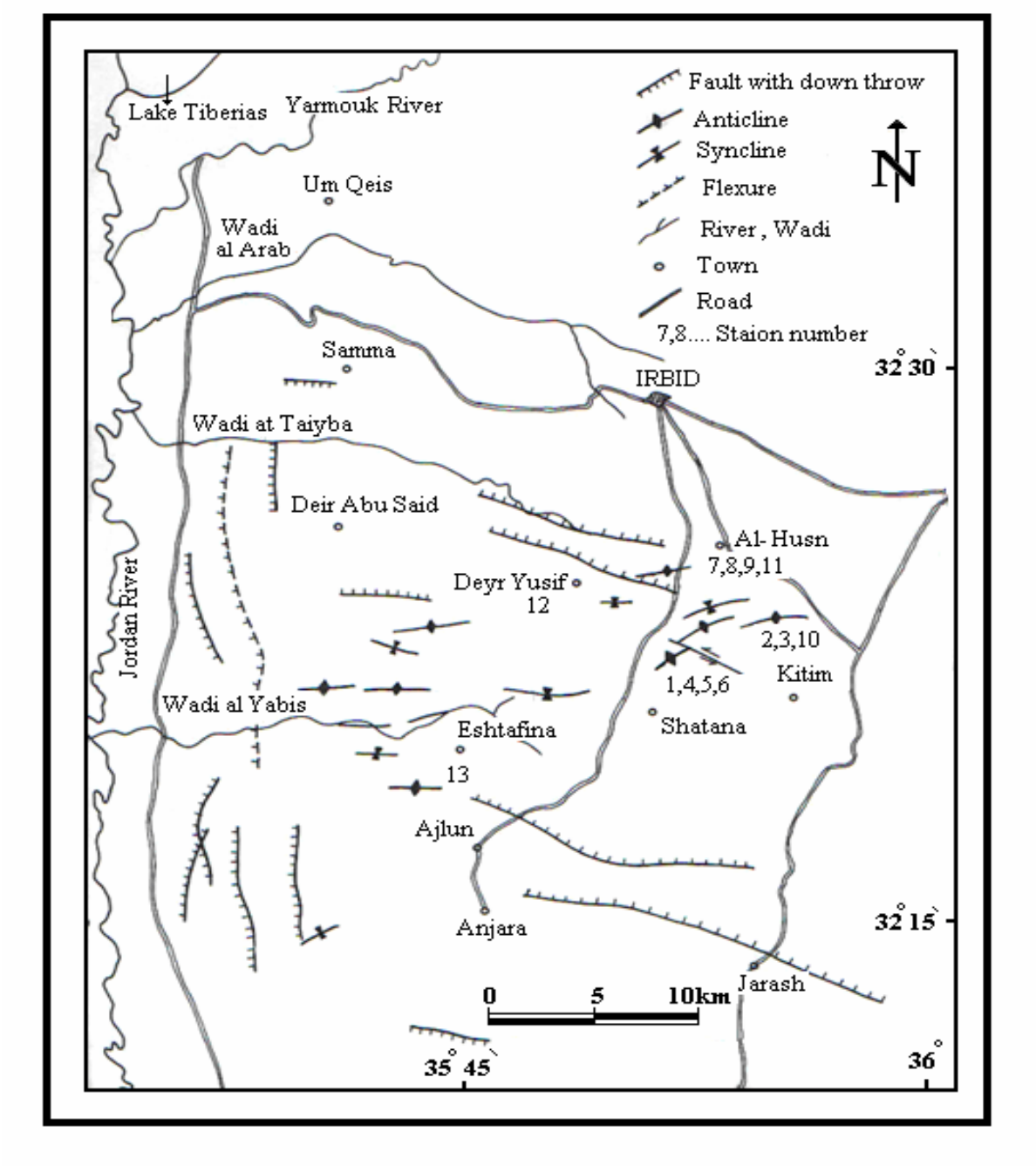

Fig.3. Major structures in northern Jordan, showing stations of fault slip data measurements.

2. Geological Setting

The outcropping rocks in the study area are of Upper Cretaceous age (Fig. 2). The oldest and most exposed rocks are the Wadi As Sir Formation of Turonian age. It is composed mostly of three distinctive parts, the lower part consists of dolomite, dolomitic limestone and/or recrystallized limestone, the middle part consists of relatively soft marly limestone and limestone, and the upper part consists almost totally of thick, bedded to massive limestone. The average thickness of this formation in the study area is 120 m (Abdelhamid, 1993). This formation is overlain by the Um Ghudran Formation of Coniacian-Santonian age, composed mainly of massive chalk at the base and intercalations of chalk and limestone at the top with chert beds and concretions. The thickness of this formation is about 30 m. The youngest rocks are the Campanian Amman Formation. It is composed of alternating beds of chert and limestone. In the study area most of this formation was eroded and remnants of fractured rocks were preserved at the top of hills.

The area of North Jordan is characterized by the presence of ENE-WSW trending Al Husn and Thaghret Asfour fold belts (Atallah and Mikbel, 1992). These fold belts occur as gentle parallel anticlines and synclines. Another prominent structure in northern Jordan is the Ajlun structure (Abed, 200. The area is cut by many faults mostly of strike slip and normal types. The general strike of these faults is WNW-ESE (Figs 2 and 3).

3. Paleostress analysis

3.1. Field Measurements

The fault slip data were collected by measuring the attitude (strike and dip) of the fault planes and the attitude (trend and plunge) of the slickenlines (lineated slickensides) on these faults. The measurements took place in 14 stations. 860 fault slip data were collected from horizontal and subhorizontal strata in the limestone quarries of the Turonian Wadi As Sir Formation. The stations are distributed in six areas in northern Jordan. Each station in most cases is one quarry, but in the case of few measurements two or more adjacent quarries were considered as one station. The attitude of slickenlines in addition to the associated features as mineral steps and tension gashes has been used to determine the orientation of slip and the sense of relative motion along the fault planes. The faults on which slickenlines were measured are generally high angle and are of normal, reverse and strike slip nature. Figure 4 shows the major trends of the fault strikes. Normal faults have two major trends: NE-SW and NW- SE, reverse faults strike NNE-SSW, dextral faults have three major trends: NE-SW, WNW- ESE, and NNW- SSE, and the sinistral faults have also three trends: NNE-SSW, E-W, and NNW- SSE.

3.2. Stress inversion method

Fault plane and slickenline orientations, including slip senses are used to compute the four parameters of paleostress tensors (σ_1, σ_2, σ_3 and R): the principal stress axis σ_1 (maximum compression), σ_2 (intermediate compression) and σ_3 (minimum compression) and the ratio of principal stress difference $R = (\sigma_2 - \sigma_3)/ (\sigma_1 - \sigma_3)$. These four parameters are determined using an improved version of the Right Dihedron method of Angelier and Mechler (1977), using the WINTENSOR computer program developed by Delvaux (2006). Paleostress inversion techniques have been used by various workers for more than 30 years. They are based upon the work of Wallace (1951) and Bott (1959), who assumed that slip on a plane occurs in the direction of the maximum resolved shear stress. The slip direction on the fault plane is inferred from slickenside lineation and calcite steps. The data used for the inversion are the fault plane, slip line orientation whereas the sense of movement was derived from slickolites and mineralization along steps for each fault plane. Stress tensors can be reconstructed by using tension and compression structures (Delvaux et al., 1995), in addition to fault planes with slip lines. Quartz veins, plume joints and dykes are considered as tension joints, developing perpendicular to the least compressive stress axis (σ_3). Fracture cleavages are considered as compression joints, developing perpendicular to the maximum compressive stress axis (σ_1). For them, the resolved normal stress magnitude is either minimized or maximized. During the rotational optimization, different functions can be optimized according to the nature of tectonic structure used. For faults, the angular deviation between observed slickensides and computed shears is minimized, together with the maximization of friction coefficients for each fault plane. Fault planes with slip lines can not only be used for the reconstruction of stress tensors, but also for tension and compression structures (Delvaux et al., 1995). The TENSOR procedure optimizes the appropriate function by progressive rotation of the tested tensor around each of its axes, and by testing different values of R. The amplitude of rotation angles and values of R ratio tested are progressively reduced, until the tensor is stabilized. Separation of fault populations resulting from successive tectonic regimes is based on interactive kinematic separation and progressive stress tensor optimization, to obtain homogeneous subsets, representing different stress regimes. Their chronological succession is established as a function of microstructural and geological criteria and in relation with known regional tectonic events (for details see Delvaux, 1993; Delvaux et al., 1995, 1997). Critical considerations on the accuracy of stress inversion methods are given in Dupin et al. (1993) and Pollard et al. (1993). They concluded that uncertainties in stress tensor determination due to geological and mechanical factors generally fall in the range of measurement errors.

The stress regime is defined by the nature of the vertical stress axes:

1) Normal faulting when σ_2 is the maximum horizontal stress axes (σ_2 SHmax) and σ_1 is vertical, 2) strike- slip faulting when σ1 is the maximum horizontal stress axes (σ1 SHmax) and when σ2 is vertical and 3) thrust/ reverse faulting when σ1 is the maximum horizontal stress axes (σ1 SHmax) and σ3 is vertical. The stress regimes also vary as a function of the stress ratio R: radial extension (σ1 vertical, $0 < R < 0.25$), pure extension (σ1 vertical , $0.25 < R < 0.75$), trans-tension (σ1 vertical , $0.75 < R < 1$ or σ2 vertical , $1> R > 0.75$), pure strike- slip (σ2 vertical , $0.75 > R > 0.25$), transpression (σ2 vertical , $0.25 > R > 0$ or σ3 vertical, $0 > R > 0.25$), pure compression (σ3 vertical, $0.25 < R < 0.75$), and radial compression (σ3 vertical , $0.75 < R < 1$) (Delvaux *et al.,* 1997).

The orientation of the principal stresses and the stress difference ratio (R) were determined by selecting those measurements of small faults with obvious sense of movement (i.e. slickolites and mineral steps).

The fourteen established stations are located on exposures of Wadi As Sir Formation. 113 measurements out of 860 were omitted because they are incompatible with slip deviations and show unreasonable results. This may be due to measurement error in the field or to local block rotation around fault blocks. Table 1 shows the number of fault- slip data used for stress tensor determination; plunge and azimuth of the principal stress axes; stress ratio; the orientation of maximum horizontal compressive stress and the deformation geometry (tensor type). Examples of stress inversion results in different sites of the study area are presented in Figure 5. Some sites like station 1 exhibit more than one tensor, indicating multiple movements (displacement) and superimposed stress states.

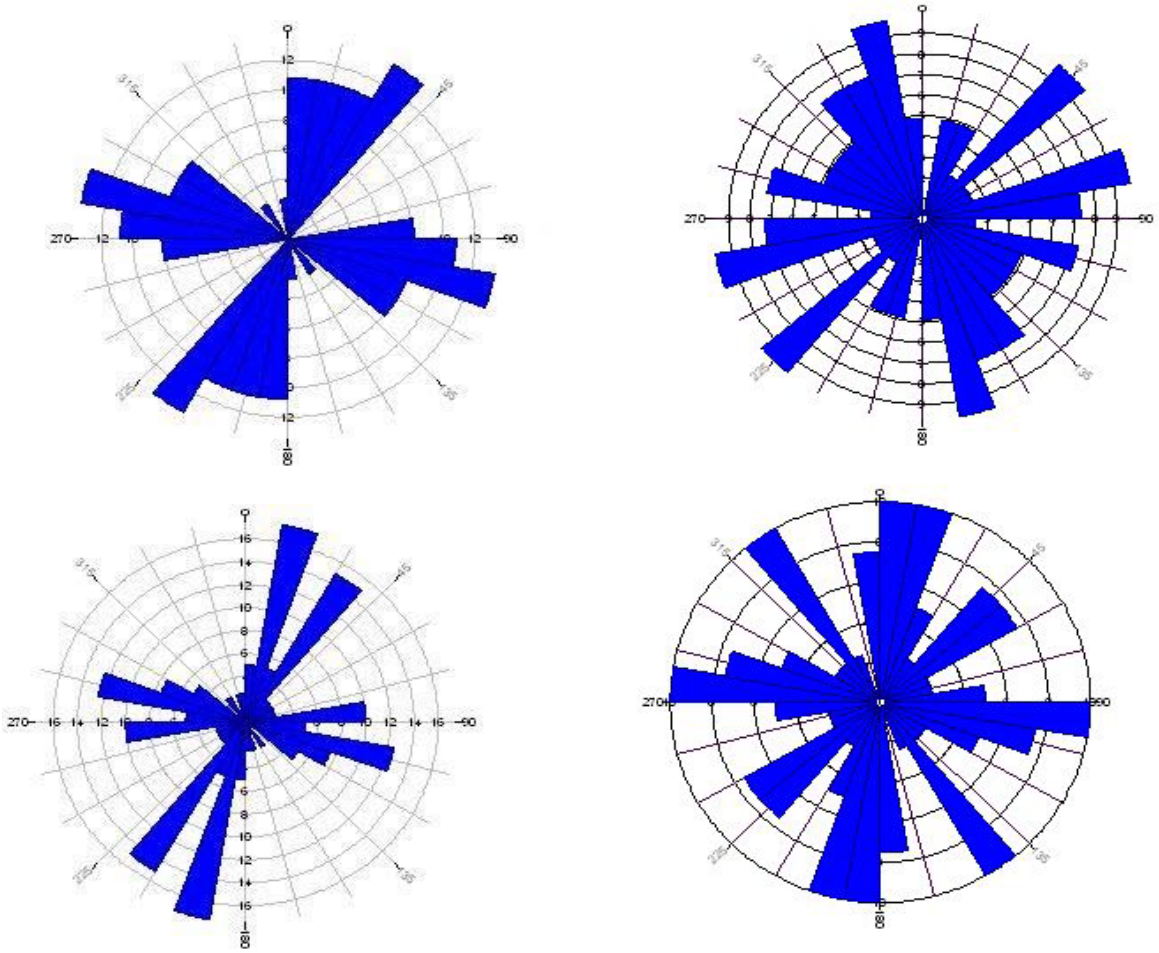

Fig. 4. General trends of fault strikes in the study area (1) normal faults (2) dextral faults (3) reverse faults and (4) sinistral faults.

4. Results

Fourteen stations have been studied in which 747 fault slip data were used in calculation. Shatana area is represented by 4 stations (1, 4, 5 and 6) , Kitim area by 3 stations (2, 3, and 10), Al-Husn area by 4 stations (7, 8, 9, and 11), and the following 3 areas by 1 station each: Deyr Yusif (station 12), Eshtafaina (station 13), and Thagret Asfour (station 14) (Figs 2 and 3).

The following is a representation of the results in each station:

4.1. Station 1

One hundred and ninety five measurements were carried out in Shatana quarries of the study area (Fig. 3 and Table 1). Two stress tensors were obtained from the whole fault population: the first stress tensor (59 measurements) gives the maximum principal stress axis (σ1) 00/ 273, the intermediate principal stress axis (σ2) 04/ 183, and the minimum principal stress axis (σ3) 85/ 315; with stress ratio(R) equals 0.21. The tensor belongs to compressive strike- slip regime. It indicates E- W compression and N- S extension. This tensor produced the conjugated WNW dextral and NNE sinistral strike- slip faults.

The second stress tensor (136 measurements) is characterized by σ1: 05/ 167, σ2: 84/ 308 and σ3: 04/ 082 with R= 0.7. This tensor belongs to pure strike- slip regime, and indicates NNW-SSE compression and ENE-WSW extension. It is responsible for the conjugated N-S sinistral and ESE dextral strike- slip faults.

4.2. Station 2

Seventy- six fault slip data were carried out in a quarry located in Kitim of the study area (Fig. 3 and Table 1). The calculated stress tensor is characterized by σ1: 25/ 065, σ2: 64/ 269 and σ3: 06/ 160 with R= 0.35. It belongs to extensive strike-slip regime and indicates ENE compression and NNW extension. This tensor show local counterclockwise rotation of the principal stress axes.

4.3. *4.3. Station 3*

Fifteen fault slip measurements have been carried out in a quarry of this station (Fig. 3 and Table 1). The resulted stress tensor is characterized by σ1: 01/ 086, σ2: 82/ 186 and σ3: 08/359 with R= 0.18. It belongs to compressive strike- slip regime and indicates E- W compression and N-S extension. This tensor produced the conjugated NE dextral and NW sinistral strike- slip faults.

4.4. Station 4

Two hundred and forty fault- slip measurements were carried out in a quarry of this station (Fig. 3 and Table 1). The stress tensor deduced from these measurements is characterized by σ1: 05/155, σ2: 80/036 and σ3: 09/243 with R= 0.52. It belongs to pure strike- slip regime and indicates NNW compression and ENE extension.

Table .1: Results of the reduced paleostress tensors from the fault-slip data

Station No.	Nt.	R	Principal Stress axis			Tensor type	S_{Hmax}
			σ_1	σ_2	σ_3		
1	59	0.21	00/273	04/183	85/315	Pure compression	273
1	136	0.7	05/167	84/308	04/082	Pure strike slip	167
2	76	0.35	25/065	64/269	06/160	Extensional strike slip	70
3	15	0.18	01/086	82/186	08/359	Compression Strike slip	89
4	240	0.52	05/155	80/036	09/243	Pure strike slip	156
5	87	0.26	03/156	22/247	68/059	Pure compression	156
6	90	0.42	11/319	78/115	04/225	Pure strike slip	135
7	35	0.65	16/155	74/316	06/068	Pure strike slip	154
8	7	0.67	03/283	85/054	09/193	Pure strike slip	103
9	15	0.7	08/091	73/201	16/000	Pure strike slip	89
10	14	0.53	81/162	05/282	04/191	Pure extension	89
11	36	0.35	71/191	09/309	16/041	Pure extension	113
12	85	0.65	77/248	16/053	03/323	Pure extension	053
13	27	0.74	70/202	11/325	24/060	Pure extension	145
14	25	0.65	03/113	83/355	06/207	Extensional strike slip	117

Nt. = net Number of measurements representing the tensor; R = stress ratio $(\sigma_2 - \sigma_3)/(\sigma_1 - \sigma_3)$; S_{Hmax} = Horizontal maximum principal stress axis.

The tensor is responsible for the WNW- trending dextral faults and the N-S sinistral faults.

4.5. Station 5

Eighty- seven fault- slip data have been carried out in this station (Fig. 3 and Table1). The tensor is characterized by σ1: 03/ 156, σ2: 22/ 247 and σ3: 68/ 059 with R= 0.26. It indicates NNW compression and belongs to pure compression regime. The tensor produced the N- S sinistral strike- slip faults and \ or the NE reverse faults at least in this station.

4.6. Station 6

Eleven fault- slip data were carried out in a quarry located in the northernmost part of the study area (Fig. 3 and Table 1).The stress tensor is characterized by σ1: 10/ 112, σ2: 76/ 247 and σ3: 10/ 020 with R= 0.45. It indicates WNW compression and NNE extension and belongs to pure strike- slip regime. This tensor is responsible for the NE- E dextral strike-slip faults.

4.7. Station 7

Ninety fault- slip measurements were carried out in this station of the study area (Fig. 3 and Table 1). The tensor is characterized by σ1: 11/ 319, σ2: 78/ 115 and σ3: 04/ 225 with R= 0.42. It indicates NW compression and NE extension and belongs to pure strike- slip regime. The tensor related with the conjugated E-W and N- S trending strike-slip faults.

4.8. Stations 8 and 9

Twenty- two fault- slip measurements were carried out in these stations (7 from station 8 and 15 from station 9). The two stress tensors are similar in the four parameters in which σ1 oriented E- W and σ3 N-S with R= 0 .7. They belong to the pure strike- slip regime (Fig. 3 and Table 1). The tensors are responsible for the conjugated ENE sinistral and WNW dextral strike-slip faults .

4.9. Station 10

Fourteen measurements were used in calculation of this station(Fig. 3 and Table 1). The resulted stress tensor is characterized by σ1: 81/ 162, σ2: 05/ 282 and σ3: 04/ 191 with R= 0.53.It indicates N- S extension and belongs to pure extension regime. This tensor is responsible for E- W trending normal faults in the study area.

4.10. Station 11

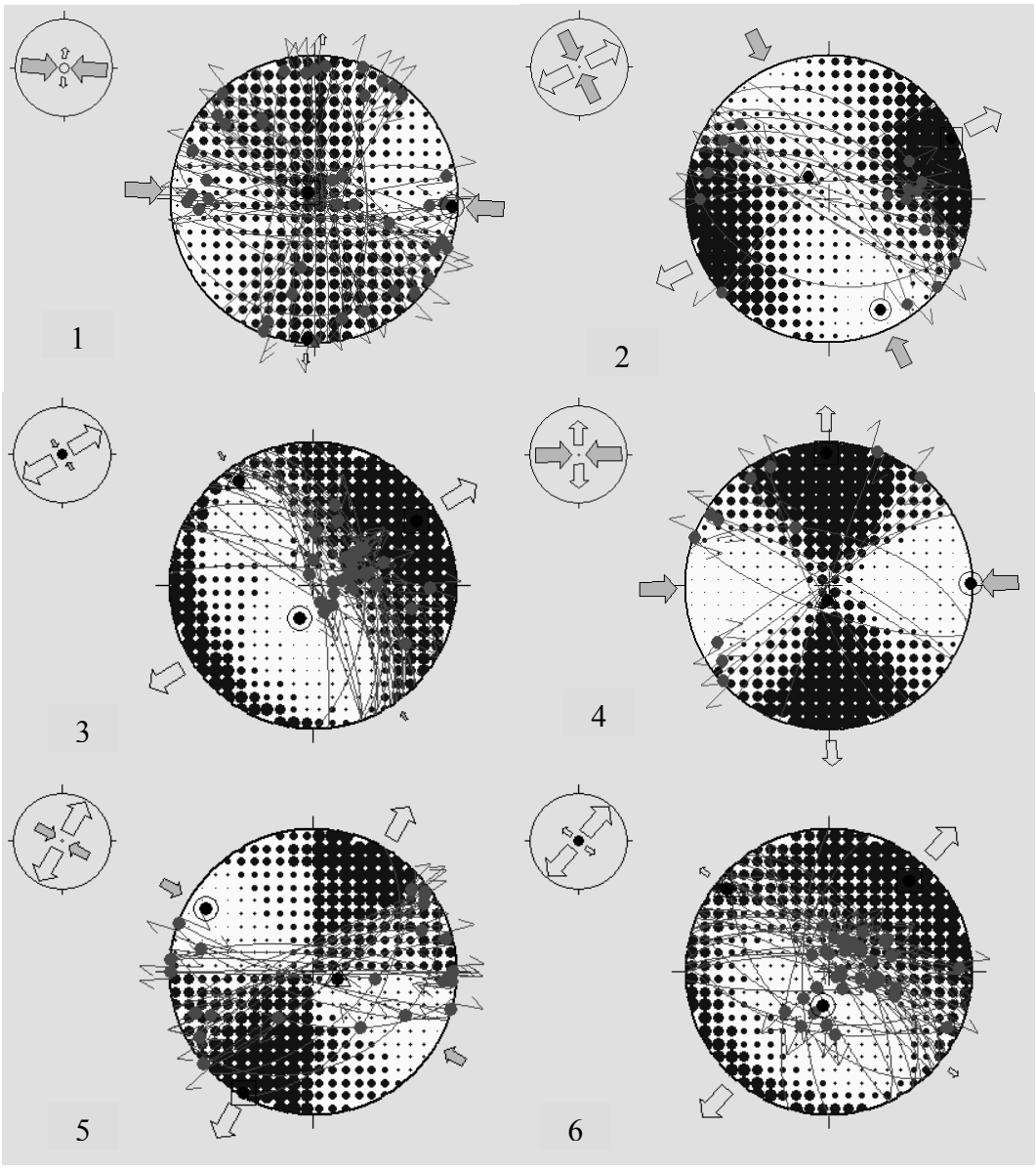

Fig. (5) Examples of stress inversion results in the different areas. (1) Shatana, (2) Kitim, (3) Deyr Yusif, (4) Al Husn, (5) Thagret Asfour, and (6) Eshtafaina.

Thirty- six were used in calculation of this station (Fig. 3 and Table 1). The resulted stress tensor is characterized by σ1: 71/ 191, σ2: 09/ 309 and σ3: 16/ 041 with R= 0.35. It indicates NE-SW extension and belongs to pure extension regime. This tensor is responsible for NW trending normal faults in the study area.

4.11. Station 12

Eighty- five fault- slip measurements were carried out in this station(Fig. 3 and Table 1). The calculated stress tensor is characterized by σ1: 77/ 248, σ2: 16/ 053 and σ3: 03/ 323 with R= 0.65. It indicates NW-SE extension and belongs to pure extension regime. This tensor shows a contra verse result.

4.12. Station 13

Twenty- seven fault- slip measurements were carried out in this station. The calculated stress tensor is characterized by σ1: 70/ 202 σ2: 11/ 325 and σ3:24/ 060 with R= 0.74. It indicates ENE extension and belongs to pure extension regime. This tensor is responsible for N- S to NNW trending normal faults in the study area (Fig. 3).

4.13. Station 14

Twenty- five fault- slip measurements were carried out in this station (Fig. 3 and Table 1). The calculated stress tensor is characterized by σ1: 03/ 113 σ2: 83/ 355 and σ3: 06 / 207 with R= 0.65. It indicates ESE compression and NNE extension. It belongs to extensional strike-slip regime. This tensor is responsible for E- W dextral strike-slip faults and to WNW trending normal faults in this station.

The above results with all parameters of the reduced stress tensors are provided in Table 1 and Fig. 5

5. Discussion and Conclusions

The data in Table 1 and Figure 5 show that, nine out of the fifteen stress tensors belong to strike -slip regime (pure

strike- slip, compressive strike- slip and extensive strike-slip). The tensors that show strike slip-dominated regimes are shown in stations 1, 2, 3, 4, 6, 7, 8, 9, and 14.

The calculated results indicate that σ1 (SHmax) and σ3 (SHmin) are generally sub-horizontal and σ2 is sub-vertical in all the previous stress tensors, which belong to a major strike-slip system with σ1 swinging around N to NW direction in stations 1, 4 ,6,and 7. These stress tensors are mainly responsible for the conjugated E- W dextral and NNW sinistral strike- slip faults in the study area. Stations 1, 3, 8, 9 ,on the other hand, show tensors with σ1 (SHmax) swinging around E- W direction. These stress tensors are mainly responsible for NNE reverse faults and conjugated NE dextral with NW sinistral faults. Four stress tensors in stations 10, 11, 12, and 13 show σ2 (SHmax), σ1 vertical and σ3 is NE oriented except station 12 shows NW extension. This situation can explain as permutation of stress axes σ1 and σ2 that occur during tectonic events and partitioned strike slip deformation. Such changes from predominantly strike- slip to predominantly normal faulting modes (σ1/ σ2 permutation) frequently occur during a single stage and a distinct stress field. Results show that both normal and strike- slip faulting have relatively stable orientation of σ3 axis, while σ1and σ2 axes may change place at a single tectonic events at spatially different regions. Two tensors in stations 1 and 5 show pure compression. The first one shows σ1 (SHmax) swinging around E- W direction, and the other shows σ1 (SHmax) swinging around NNW- SSE direction. This means that they belong to two different stress systems and are compatible with the regional known stress fields in the region.

Figure 5 and Table 1 show the reduced stress tensors with the orientation of both the horizontal maximum stress axes (Sh_{max}) and the horizontal minimum stress axes (Sh_{min}). The orientation of stress tensors in the different areas can be summarized in the following trends:

1. Six stations show a NW to NNW compression and NE to ENE extension. These tensors related with the Dead Sea stresses during the Miocene and the later stages.
2. Three stations show an E-W to ESE compression and N-S to NNE extension. These tensors are related with the Syrian Arc Stress field and responsible for the formation of the associated conjugated ENE- WSW dextral and NW-SE sinistral strike-slip faults in the study area.
3. Two stations show orthogonal pure compression (E- W and NNW- SSE). These tensors explained as the reactivation of the Syrian Arc related structures by the Dead Sea stresses on Post- Miocene times.
4. Three stations have a NE-SW extension. These stress tensors may be responsible for the formation of the local E-W and ESE- WNW normal faults in the study area. These stress tensors include three paleostress regimes, one with predominantly strike slip faulting (strike slip regime) and the two others with predominantly dip slip either normal faulting (extensional regime) or dip slip reverse faulting (compression regime).

There are some paleostress studies in the region. The work of Eyal and Reches (1983), Ron and Eyal (1985), Eyal (1996), and finally Eyal et al (2001) west of the DST show that, there are two main stress fields acting on the area since the Late Cretaceous, the oldest is the E-W to ESE-WNW compression. According to these authors, this stress is responsible for the formation of the Syrian Arc belt and they call this stress the Syrian Arc System (SAS). The second younger stress system is the N-S to NNW-SSE compression, and is responsible for the 105 km sinisitral displacement along the DST and the opening of the Red Sea since the Miocene, it is called the Dead Sea System (DSS). East of the rift , the work of Diabat (1999), Diabat et al (2004), and Zain Eldeen et al (2002) found almost the same above mentioned stress systems in addition to other local stresses. In the present study, the most dominating stress system is the NW to NNW compression, this stress system is compatible with the DSS. The second stress is the E-W to ESE compression, which is compatible with the SAS. The stations which have N-S and NE-SW extension are characterized by vertical σ_1. These stress tensors may be responsible for the formation of the E-W and the ESE- WNW normal faults shown on the map of Figure 3.

References

Abed, A. 2000. Geology of Jordan. Publication of Jordanian Geologists Association.

Abdelhamid, GH. 1993. Geological map of Jerash, scale 1: 50000. Geological mapping division, NRA, Jordan.

Angelier, J. 1979. Determination of the mean principal stresses for a given fault population. Tectonophysics 56: T17-T26.

Angelier, J. 1989. From orientation to magnitudes in paleostresses determinations using fault slip data. J. Struct. Geol. 11:37-50.

Angelier, J. 1994. Fault slip analysis and paleostress reconstruction. In Hancock , P. (ed): continental deformation. Pp: 53-100, Pergamon Press Oxford.

Angelier, J. and Mechler, P. 1977. Sur une method graphique de recherché des contraintes principals egalement utilizable en techtonique et en seismologie: la method de diedres droils. Bull. Soc. Geol. Fr. 7: 1309-1318.

Atallah, M.,1992. On the structural pattern of the Dead Sea Transform and its related structures in Jordan. Abhath Al-Yarmouk (Pure Sciences and Engineering) 1, 127-143.

Atallah, M. and Mikbel, Sh. 1992 structural analysis of the folds between Wadi El Yabis and the basalt plateau, northern Jordan. Dirasat 19B: 43-58.

Ben- Avraham, Z., Almagor, G., Garfunkel, Z.,1979. Sediments and structures of the gulf of Elat. Sediment. Geol. 23, 239- 267.

Bender, F., 1968. Geology of Jordan. Borntraeger, Berlin. 196 p.

Bott, M.H.P., 1959. The mechanism of oblique slip faulting. Geological Magazine 96, 109-117.

Burdon, D. J., 1959. Handbook of the Geology of Jordan: to accompany and explain the three sheets of 1: 250,000 Geological Map, East of the Rift, A. M.

Chu, D., Gordon, R. G., 1998. Current plate motions across the Red Sea. Geophys. J. Int. 135, 313- 328.

Delvaux, D. 1993. TENSOR program for paleostress reconstruction: examples from the East Africa and the Baikal Rift Zones. EUGVII Strassbourg, France , Terra Nova 5, 216.

Delvaux, D. 2006. WINTENSOR, VERSIO 1.3.75, Royal Museum for Central Africa, Tervuren, Belgium Dept. Geology – Mineraolgy.

Delvaux, D. Moeys, R., Stapel, G., Melnikov, A., and Ermikov, V. 1995. Paleostress reconstructions and geodynamics of the Baikal region, central Asia, Part I. Paleozoic and Mesozoic pre-rift evolution. Tectonophysics 252:61-101.

Delvaux, D. Moeys, R., Stapel, G., Petit, C., Levi, K., Miroshnichenko, A., Ruzchich, V., and San'kov, V. 1997. Paleostress reconstructions and geodynamics of the Baikal region, Central Asia, Part 2. Cenozoic rifting. Tectonophysics 282:1-38.

Diabat, A. 1999. Paleostress and strain analysis of the Cretaceous Rocks in the Eastern Margin of the Dead Sea Transform, Jordan. Unpublished Ph.D Thesis, University of Baghdad.

Diabat, A., 2002. Strain analysis of the Cretaceous rocks in the Eastern margin of the Dead Sea Transform, Jordan. Dirasat 29, 159-172.

Diabat, A., Salih, M., and Atallah, M., 2003. Magnitudes of the paleostresses at the Eastern Rim of the Dead Sea Transform Fault,Jordan. Dirasat, 30, 1-18.

Diabat, A. Masri, A.. 2005. Orientation of the principle stresses along Zarqa-Ma'in fault. Muta Journal for Researchs and studies 20: 57-71.

Diabat, A. Atallah, M., Saleh, M. 2004. Paleostress analysis of the Cretaceous rocks in the eastern margin of the Dead Sea transform, Jordan. Journal of African Earth Sciences 38: 449-460.

Dupin, G. M., Sassi, W., Angelier, J.., 1993. Homogeneous stress hypothesis and actual fault slip: a distinct element analysis. Journal of Structural Geology 15, 1033- 1043.

Eyal, Y. 1996. Stress fluctuation along the Dead Sea rift since the Middle Miocene. Tectonics 15:157-170.

Eyal, Y., Reches, Z., 1983. Tectonic analysis of the Dead Sea Rift region since the Late Cretaceous based on mesostructures. Tectonics 2:167- 185.

Eyal, Y., Gross, M., Engelder. T., Backer,A. 2001. Joint development during fluctuation of the region stress field in southern Israel. Journal of Structural Geology 23:279- 296.

Garfunkel. Z. 1981. Internal structure of the Dead sea leaky transform (rift) in relation to plate kinematics. Tectonophysics 80: 81-108.

Freund, R., Zak, I., Garfunkel, Z., 1968. Age and rate of the sinistral movement along the Dead Sea rift. Nature 220, 253- 255.

Garfunkel, Z., 1981. Internal structure of the Dead Sea leaky transform (rift) in relation to plate kinematics. Tectonophysics 80, 81- 108.

Joffe, S., Garfunkel, Z., 1987. Plate kinematics of the circum Red Sea. A re- evaluation. Tectonophysics 141, 5- 22.

Klinger, Y., Avouac, J.P., Abou Karaki, N., Dorbath, L, Bourles, D., Reyss, J. L., 2000a. Slip rate on the Dead Sea transform fault in northern Araba valley. Geophys. J. Int. 142, 755- 768.

Klinger, Y., Avouac, J.P., Dorbath, C, Abou Karaki, N., Tisnerat, N., 2000b. Seismic behavior of the Dead Sea fault along Araba valley, Jordan. Geophys. J. Int. 142, 769- 782.

McKenzie, D., Davies, D., Molnar, P., 1970. Plate tectonics of the Red Sea and East Africa. Nature 226, 243- 248.

Mikbel, Sh., 1986. Some relevant tectonical and geotechnical considerations of south Amman area/ Jordan.. Dirasat 7, 215-225.

Mikbel, Sh., Zacher, W., 1981. The Wadi Shueib structure in Jordan. Neues Jaharbuch fuer Geologie und Paleontologie Monatshefte 9, 571-576.

Pollard, D. D., Saltzer, S. D., Rubin, A., 1993. Stress inversion methods: are they based on faulty assumption ?. Journal of Structural Geology 15 (8) , 1045- 1054.

Quennell, A.M., 1983. Evolution of the Dead Sea Rift. A review, First Jordanian Geologic Conference 460-482.

Ron, H., Eyal, Y. 1985. Intraplate deformation by block rotation and mesostructures along the Dead Sea transform, northern Israel. Tectonics 4 :85-105

Salameh, E. Zacher, W. 1982. Horizontal stylolites and paleostress in Jordan. N.Jb, Geol.Palaont, Mh. 1982: 509-512.

Shapira, A., Hofstetter, H., 1993. Source parameters and scaling relationships of earthquakes hn Israel. Tectonophysics 217, 217-226.

Wallace, R.E., 1951. Geometry of shearing stress and relation to faulting. Journal of Geology 59, 118- 130.

Zain Eldeen, U. Delvaux, D. and Jacobs. J. 2002. Tectonic evolution in the Wadi Araba segment of the Dead Sea rift, southwest, Jordan. EGU Stephan Mueller special publication series, 2: 63-81.